

# Effect of Spoiler Angle on the Aerodynamic Performance of Hatchback Model

Cheng See Yuan<sup>1,2\*</sup>, Shuhaimi Mansor<sup>3</sup> and Mohd Azman Abdullah<sup>1,2</sup>

<sup>1</sup>Centre for Advanced Research on Energy, UTeM, Hang Tuah Jaya, 76100 Durian Tunggal, Melaka, Malaysia.

<sup>2</sup>Faculty of Mechanical Engineering, UTeM, Hang Tuah Jaya, 76100 Durian Tunggal, Melaka, Malaysia.

<sup>3</sup>Faculty of Mechanical Engineering, UTM, 81310 UTM Skudai, Johor, Malaysia.

\*Correspondence Author

## Abstract

Rear spoiler is a device commonly found on road vehicles for improving their aerodynamic performance. The main aim of the present study was to investigate the effect of varying the spoiler angle on the aerodynamic performance of hatchback vehicles. A simplified road vehicle model was used to facilitate the investigation. The study utilized a RANS-based computational fluid dynamics (CFD) method. As for the purpose of validating the method, the numerically obtained results was compared to the experimental data. The numerical result shows that at positive spoiler angle, the aerodynamic lift of the hatchback model has reduced dramatically – up to 2937%. However, the spoiler effect is unfavorable to lift reduction when configured at negative inclination angle. Although the aerodynamic lift was found to decrease with the increase in spoiler angle, there is accompanied by a drag penalty. Finally, the physical mechanism was discussed based on flow visualization results.

**Keywords:** Rear spoiler, spoiler angle, aerodynamics, hatchback, CFD

## INTRODUCTION

A properly designed rear spoiler can reduce the rear-axle lift of a vehicle. This effect is important because a vehicle with its rear-axle lift lower than the front exhibits better stability, i.e. requires minimum driver intervention to maintain a straight path [1]. In addition, when a vehicle makes a turn, it needs sufficient traction to provide the centripetal force for it to pass the curve without slip. Hence, the use of spoiler will enable the vehicle to achieve greater downforce (negative lift), and thus better traction without significant increase in its weight.

There are two types of rear spoiler design: strips and free-standing wing. The effectiveness of wing-type spoiler has been reported in numerous studies. For instance, Tsai et al. [2] investigated numerically five different spoiler configurations. The spoilers are of inverted airfoil type and were mounted on the trunk of a simplified car model based on the HONDA S2000. Although all the cases had shown reduction in lift, however, only one out of five configurations succeeded in

producing a negative lift coefficient value.

Meanwhile, Daryakenari et al. [3] has shown a similar trends. Its numerical results indicate that up to 75% reduction in lift coefficient for a passenger car model can be achieved by properly manipulating the inclination angle of its flat-plate-type spoiler, i.e. at 50° relative to the ground. Similarly, Kodali and Bezavada [4] has observed a decrease of 80% lift coefficient in the case of a simplified-passenger-car model mounted with an inverted-airfoil type spoiler.

As for strip-type rear spoilers, Menon et al. [5] has investigated the influence of spoiler on the aerodynamic drag and crosswind stability of a simplified hatchback model, namely, an Ahmed model at 35° slant angle. Although these two performances are important, the study did not cover aerodynamic lift performance which is important for driving stability. Moreover, extensive literature search found that the coverage of this particular topic – strip-type rear spoiler's influence on lift performance – is scarce. To fill the gap, hence, the main objective of the present paper is to investigate the effect of strip-type rear-roof spoiler on the aerodynamic lift performance of simplified hatchback model.

## METHODOLOGY

### Hatchback Model And Spoiler Configurations

The Ahmed body which represents simplified road vehicle geometry in the form of a bluff body was adopted. The slant angle was at 35° (see Figure 1), which is typical for most hatchback cars. Figure 2 shows the convention of the spoiler angle  $\alpha$ . As illustrated,  $\alpha$  is the angle between the horizontal and the upper face of the spoiler. Positive angles are measured counterclockwise from horizontal. Note that the solid line is the profile of the spoiler at  $\alpha = 15^\circ$ . Meanwhile, the dashed lines are the spoiler profiles at  $\alpha = -15^\circ, 0^\circ, 5^\circ$ , and  $10^\circ$ , respectively. For all configurations, the length of the spoiler was fixed at 66.6 mm, which corresponds to 30% of the length of the slant section. The trailing edge of the spoiler was filleted (5 mm radius) to avoid highly skewed cells during meshing. For the same reason, the angle between the slant section and the rear face of the spoiler was maintained at right

angle for all configurations. For details of the Ahmed model dimensions, the reader is referred to Ahmed [6, 7].

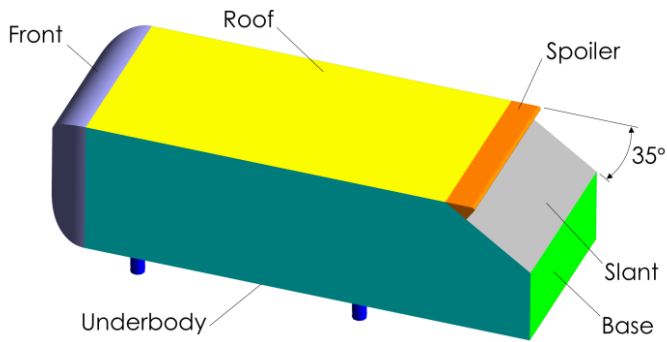


Figure 1: Ahmed model fitted with a rear-roof spoiler

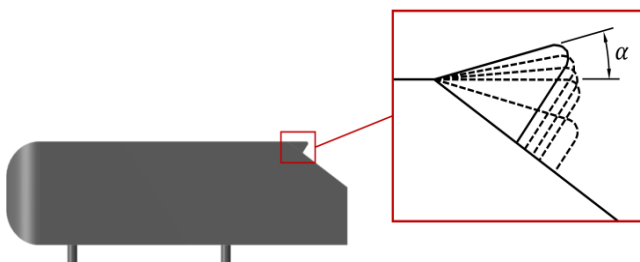


Figure 2: Convention of spoiler angle

## COMPUTATIONAL METHOD

### CFD Settings

The present study employed a numerical simulation method to investigate the influence of rear spoiler angle on the aerodynamics forces of a simplified hatchback model. All results were obtained using the commercial CFD finite-volume solver by ANSYS. Note that the ANSYS's CFD solver has well been validated for wide range of applications such as in sport (e.g. [8]), medical (e.g. [9]), combustion (e.g. [10]), heat transfer (e.g. [11, 12]), urban aerodynamics (e.g. [13]), automotive (e.g. [14, 15]), etc. The Reynolds-averaged Navier-Stokes (RANS) approach was used. The turbulence model was the widely used two-equation model, namely, k-epsilon realizable model with enhanced wall treatment. The steady, pressure-based solver was utilized to achieve steady-state simulations. All reported results were obtained using a second-order node-based upwinding discretization scheme.

The inlet boundary condition was set as uniform flow with  $U = 40$  m/s and the turbulence intensities of 0.2%. The corresponding Reynolds number (Re) was 768,000 based on the model height. As for the outlet boundary, the pressure outlet at zero gauge pressure was imposed. The side and top walls of the domain was defined as symmetry boundary condition. Meanwhile, the ground and model surfaces were set as no-slip wall.

The computational domain resembles a rectangular box. Since

the model is symmetric and the flow is steady, all simulation cases were run for half of the flow domain with a symmetry plane placed at the centerline location. The cross sectional area of the half flow domain was 1738 mm x 1129.5 mm (height x width). The corresponding blockage ratio was less than 1.5%, which is well within the typically accepted range of 5% in automotive aerodynamic testing [16]. The upstream and downstream extends of the domain were 1.4 and 11.4 times the model length, respectively.

### Meshing

The computational domain was decomposed into unstructured and prismatic cells (see Figure 3). The latter was employed around the model and the ground for improving the boundary layer resolution. The first prismatic cell layer thickness around the model surface was at 0.5 mm. The corresponding  $y^+$  ranges from around 1 to 57, which is within the appropriate range for employing the k-epsilon turbulence model. The total nodes and cells for all simulation cases were around 315,000 and 890,000, respectively.

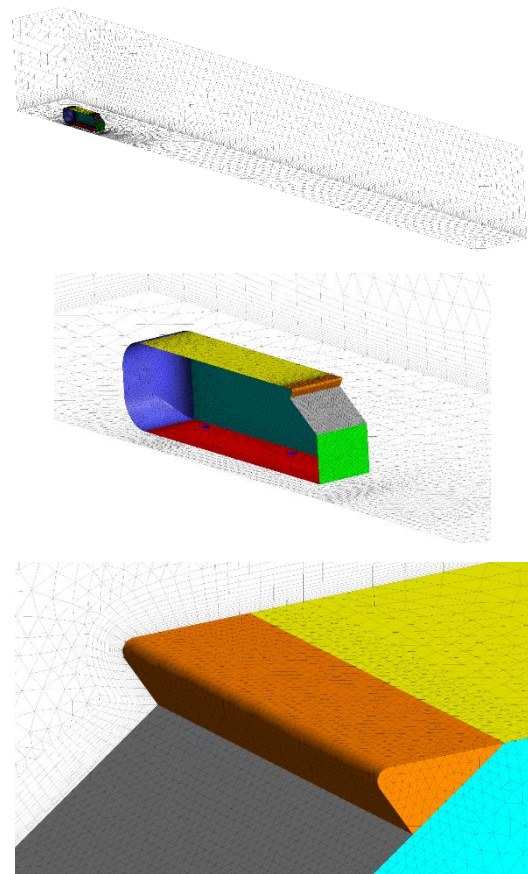
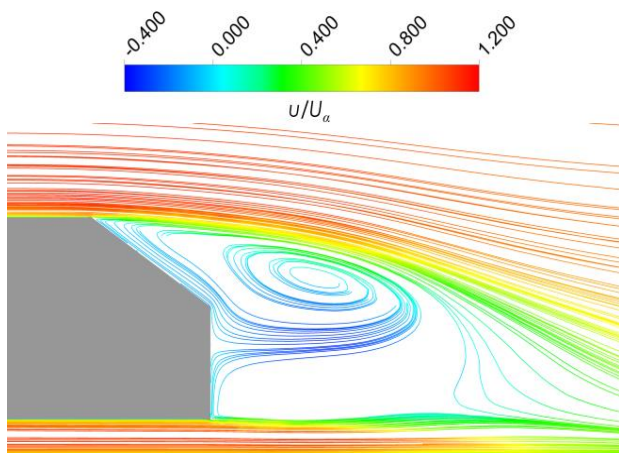


Figure 3: Numerical cells of the simulation domain (top), surface mesh of the model (middle), and close-up of prismatic cells around the rear-roof spoiler (bottom)

## Validation

Validation of the numerical method was carried out by comparing the numerically obtained results of Ahmed model without the spoiler to the experimental results found in the literature. The Re was at 768,000 (based on the model height) which was consistent with the experimental Re of Lienhart et al. [17]. Figure 4 shows the flow features at the rear section of Ahmed model along the centerline reproduced by the present simulation. As depicted, the flow separates from the roof-backlight junction. It does not reattach at the slanted edge, but continues downstream and joins the separation bubble trailing the vertical base of the model. Qualitatively, this flow pattern is consistent with the experimental results reported in numerous literature (e.g. [6, 17, 18]).



**Figure 4:** Flow streamlines around the rear section of the model in the symmetric plane colored by the magnitude of normalized streamwise velocity component

Table 1 compares the drag coefficient  $C_d$  values obtained from the present study to the experimental data by Lienhart et al. [17]. As shown, the total  $C_d$  value was in excellent agreement with the experiment, i.e. percentage difference of 3.44%. The drag breakdown shows that the  $C_d$  of the base and slant sections were well predicted. Good prediction of  $C_d$  in these two sections is important because the influence of the spoiler was expected to be most prominent at the rear section.

**Table 1:** Comparison of the experimental  $C_d$

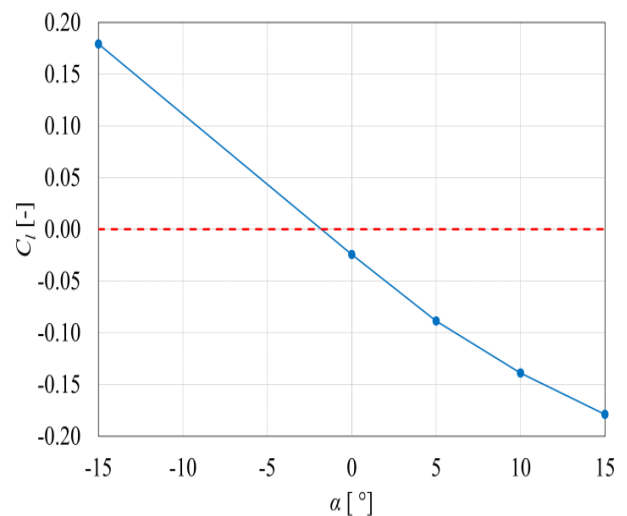
Source	CFD (present)	Exp. [8]	Percentage diff. (%)
Slant	0.095	0.097	2.08
Base	0.094	0.090	4.35
Front	0.039	0.015	88.89
Viscous	0.038	0.055	36.56
Total	0.0265	0.0257	3.44

## RESULTS AND DISCUSSION

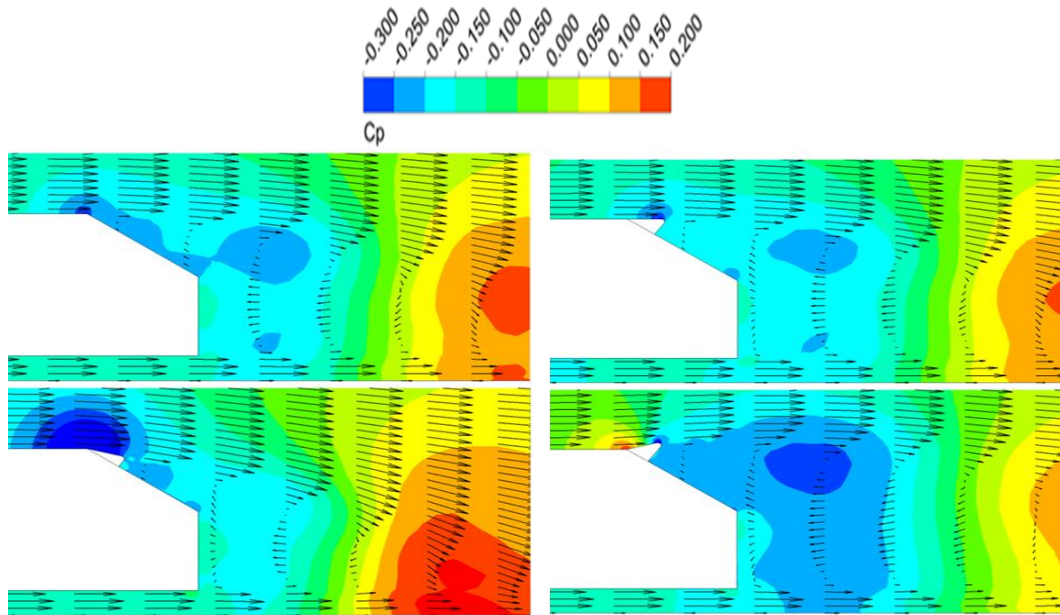
### Effects of rear spoiler angle $\alpha$

Figure 5 shows that the lift coefficient  $C_l$  decreased almost linearly with  $\alpha$  for the range of  $\alpha$  tested. In addition, it is evident that the benefit of fitting a spoiler only occurred at positive  $\alpha$ . At negative  $\alpha$ , relatively higher  $C_l$  was found, which is deemed unfavorable to driving stability.

Figure 6 compares the distribution of static pressure coefficient  $C_p$  (colour contour) and streamwise velocity component (vectors) around the rear section of the model at different spoiler configurations. In general, the flow at the upper body separated near the trailing edge of the roof when without the spoiler, whereas, it separated near the end of the spoiler for all spoiler angles when a spoiler is used. Besides, when a spoiler was configured at zero or positive  $\alpha$ , it prevented the flow from accelerated near the roof-backlight junction. Thus, resulted in a higher static pressure around the junction. As for the spoiler with negative  $\alpha$ , augmentation of flow occurred near the junction, and was accompanied by significant drop in static pressure.



**Figure 5** Graph of  $C_l$  against rear spoiler angle  $\alpha$ ; Dashed-horizontal line is without spoiler



**Figure 6:** Vectors of streamwise velocity component and  $C_p$  distribution along the symmetry plane at the rear section of the model; Without spoiler (top),  $\alpha = -15^\circ$ ,  $0^\circ$ , and  $15^\circ$  (bottom left and all on right)

Meanwhile, as depicted in Figure 6, the spoiler angle also has an effect on the size of the separation bubble behind the model. As shown, the height and length of the separation bubble are found to increase with larger spoiler angle.

Figure 7 compares the effect of spoiler angles on the  $C_p$  distribution along the centerline of the model. As expected, the  $C_p$  at the front section is almost identical in all cases. However, from the midsection onward, deviations in  $C_p$  are gradually becoming more apparent along the upper body. The  $\alpha = 0^\circ$  and  $15^\circ$  cases exhibited higher  $C_p$ , with the latter being more pronounced, as compared to the case without a spoiler. Whilst, the  $\alpha = -15^\circ$  case shows a significant drop in  $C_p$  particularly around the rear end of the roof, and the value peaked at the roof-spoiler junction.

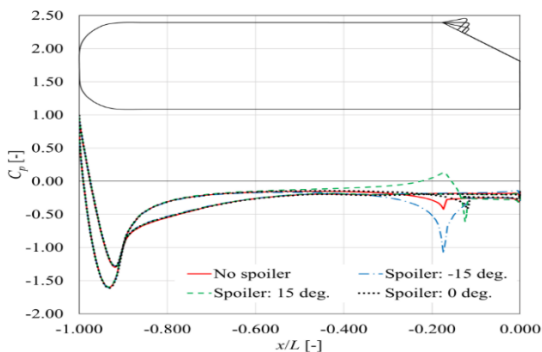


**Figure 7**  $C_p$  distribution along the centerline of four cases: Without spoiler (solid curve); with spoiler,  $\alpha = 0^\circ$  (dotted curve),  $15^\circ$  (dashed curve), and  $-15^\circ$  (dashed-dotted curve)

In general, the spoiler affects the aerodynamic lift of the model mainly by altering the flow near the rear end of the roof

where the spoiler was mounted (see Figure 7 and 8). At  $\alpha = 0^\circ$ , the relatively higher surface pressure near the rear end of the roof has caused significant reduction in  $C_l$  (by about 488%) as compared to the case without the spoiler. In addition, the  $C_d$  has reduced by about 3% (see Figure 8). Note that this positive combination – reduction in both the drag and lift – is highly appreciable as it is often the case that the element that increases the downforce will also increase drag (e.g. [2-4]).

At  $\alpha = 15^\circ$ , significant increase in the surface pressure near the roof-spoiler junction may be evident (see Figure 8). This high pressure region has resulted in the dramatic drop in  $C_l$ , by about 2937%. However, it was accompanied by about 11%  $C_d$  increment. Hence, this configuration might not be suitable in situations where fuel economy is important.

At negative  $\alpha$  (i.e. the  $-15^\circ$  case), the airflow around the roof-spoiler junction accelerated downward with the corresponding drop in the model's surface pressure around the region. Therefore, the  $C_l$  has increased (by about 2737%).

Although increasing the spoiler angle leads to lower  $C_l$ , however, Figure 9 shows that in general, the  $C_d$  would increase. Therefore, lift reduction practice has to be carried out with care so as not to introduce significant drag increment. Particularly in cases where drag performance is important such as in hybrids and EVs. This could be the reason why the use of rear-roof spoiler at high  $\alpha$  (above  $5^\circ$ ) is scarce in commercial vehicles as their need for downforce is not as crucial as in race cars.

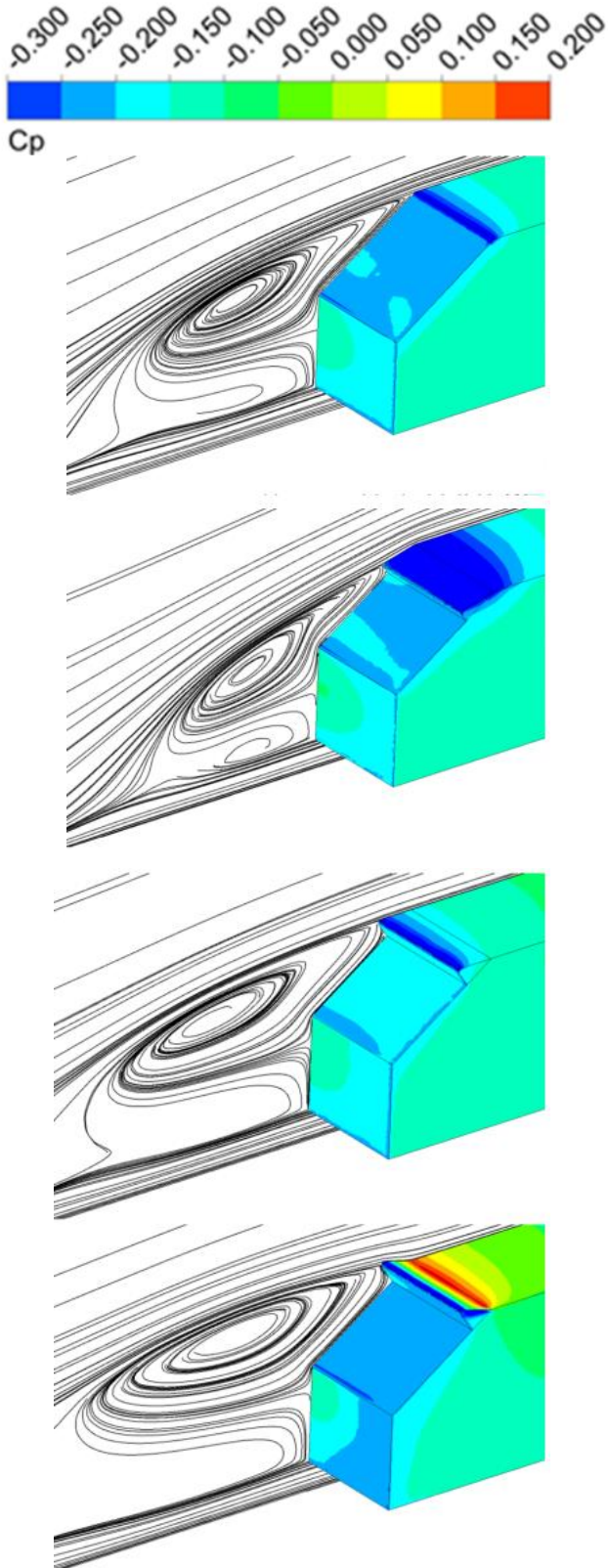


**Figure 8:** Surface pressure distribution around the rear section of the model and the streamlines along the symmetry plane; Without spoiler (top left),  $\alpha = -15^\circ$  (bottom left),  $0^\circ$  (top right), and  $15^\circ$  (bottom right)

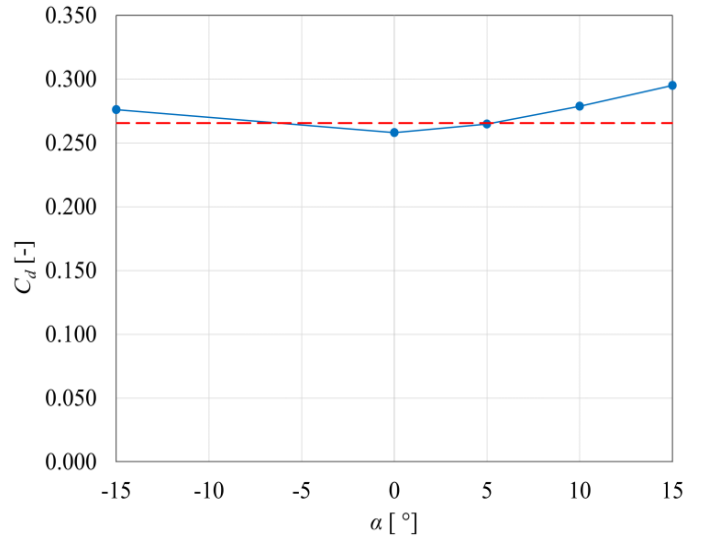


**Figure 9** Graph of  $C_d$  against rear spoiler angle  $\alpha$ ; Dashed-horizontal line is without spoiler

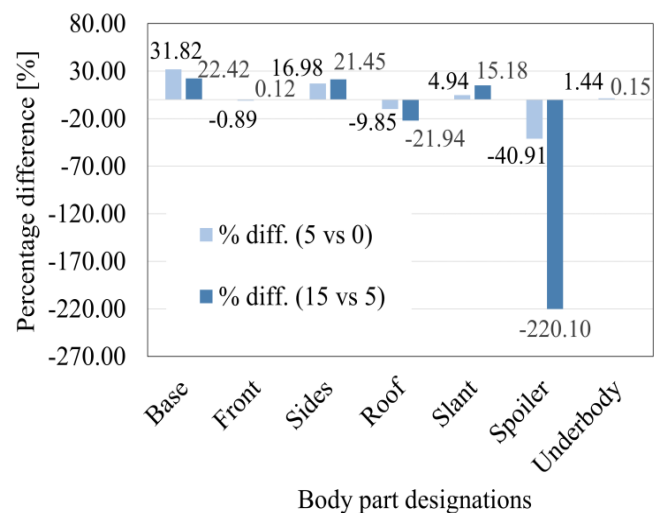


**Figure 10** Percentage difference in  $C_i$  per body part as  $\alpha$  increases from  $0^\circ$  to  $5^\circ$  (left bar), and from  $5^\circ$  to  $15^\circ$  (right bar)

### Body part contribution to $C_i$ reduction

Figure 10 compares the percentage difference of  $C_i$  per body part as  $\alpha$  increases from  $0^\circ$  to  $5^\circ$ , and from  $5^\circ$  to  $15^\circ$ . As depicted, the decrease in  $C_i$  was mainly come from the spoiler and roof. This result supports the qualitative discussions pertaining to Figure 8.

### CONCLUSIONS

This paper investigated the effect of strip-type rear-roof spoiler on the aerodynamic performance of hatchback vehicles

by a RANS-based CFD method. The results show that the aerodynamic lift was to decrease nearly linearly with the inclination angle of the spoiler, and was accompanied by the increment in aerodynamic drag. However, it is possible to achieve reduction in both the lift and drag when the spoiler is configured at  $0^\circ$  - parallel to the roof. In contrast, at negative spoiler angle, the use of rear spoiler was counterproductive to both the lift and drag reductions. In addition, when a spoiler is used, apart from the spoiler itself, the main body part that has contributed to the lift reduction was the model's roof, particularly at the rear end where the spoiler was mounted.

The present results were obtained from stationary simulations in which the motion of vehicle body was not considered. In practice, motion of vehicle body is very common and could change the inclination angle of the spoiler when the motion mode is of pitching. Hence, it helps to provide insight into how each spoiler configurations would perform under a more realistic driving condition if certain motion mode could be incorporated in the flow simulation. For this purpose, the method introduced by Cheng et al. [19, 20] could be employed in the future studies.

#### ACKNOWLEDGEMENT

The authors would like to thank Universiti Teknikal Malaysia Melaka (UTeM) and Ministry of Higher Education for supporting this research under FRGS FRGS/1/2015/TK03/FKM/02/F00273.

#### REFERENCES:

- [1] Howell, J. and Le Good, G. 1999. The influence of aerodynamic lift on high speed stability. SAE Paper No 1999-01-0651.
- [2] Tsai, C. H., Fu, L. M., Tai, C. H., Huang, Y. L. and Leong, J. C. 2009. Computational aero-acoustic analysis of a passenger car with a rear spoiler. *J. Appl. Math. Model.* 33(9): 3661-3673.
- [3] Daryakenari, B., Abdullah, S., Zulkifli, R., Sundararajan, E. and Mohd Sood, A. 2013. Numerical study of flow over ahmed body and a road vehicle and the change in aerodynamic characteristics caused by rear spoiler. *Int. J. Fluid Mech. Res.* 40(4): 354-372.
- [4] Kodali, S. P. and Bezavada, S. 2012. Numerical simulation of air flow over a passenger car and the influence of rear spoiler using CFD. *IJATP.* 01(1): 6-13.
- [5] Menon, D. P., Kamat, G. S., Mukkamala, Y. S. and Kulkarni, P. S. 2014. To improve the aerodynamic performance of a model hatchback car with the addition of a rear roof spoiler. 16th Annual CFD Symposium.
- [6] Ahmed, S. R. 1981. An experimental study of the wake structures of typical automobile shapes. *J. Wind Eng. Ind. Aerodyn.* 9(1-2): 49-62.
- [7] Tunay, T., Sahin, B., and Ozbolat, V. 2014. Effects of rear slant angles on the flow characteristics of Ahmed body. *Experimental Thermal and Fluid Science.* 57: 165-176.
- [8] Jahi, T. M., Zawawi, H. I., and Rahman, N. A. 2015. Effect of skirt angle and feathers formation on shuttlecock aerodynamics performance. *Jurnal Teknologi.* 76(8): 95-99.
- [9] Missel, P. J., Horner, M., and Muralikrishnan, R. 2010. Dissolution of intravitreal triamcinolone acetamide suspensions in an anatomically accurate rabbit eye model. *Pharm Res.* 27: 1530-1546.
- [10] Torabmostaedi, H., Zhang, T., Foot, P., Dembele, S., and Fernandez, C. 2013. Process control for the synthesis of ZrO<sub>2</sub> nanoparticles using FSP at high production rate. *Powder Technology.* 246: 419-433.
- [11] Abd Munir, F., Mohd Azmi, M. I., Razali, N., Mat Tokit, E. 2012. The Effect of Parameter Changes to the Performance of a Triangular Shape Interrupted Microchannel Heat Sink. *Jurnal Teknologi.* 58(2): 33-37.
- [12] Alawi, O. A., Che Sidik, N. A., and Wah, Y. T. 2015. A numerical study of heat transfer to turbulent separation nanofluid flow in an annular passage. *Jurnal Teknologi.* 77(8): 75-82.
- [13] Cheng, S.Y. 2007. The effect of building shape modification on wind pressure differences for cross-ventilation of a low-rise building. *International Journal of Ventilation.* 6(2): 167-176.
- [14] Ahmad Shafie, N. E., Mohamed Kamar, H. and Kamsah, N. 2015. Effects of ventilation setups on air flow velocity and temperature fields in bus passenger compartment. *Jurnal Teknologi.* 77(30): 49-53.
- [15] Ahmad Shafie, N. E., Mohamed Kamar, H. and Kamsah, N. 2015. A cfd simulation of pm1 and co air contaminants in a bus passenger compartment. *Jurnal Teknologi.* 77(30): 35-39.
- [16] Hucho, W-H. and Sovran, G. 1993. Aerodynamics of road vehicles. *Annu. Rev. Fluid Mech.* 25: 485-537.
- [17] Lienhart, H., Stoots, C. and Becker, S. 2000. Flow and turbulence structures on the wake of a simplified car model (Ahmed model). *DGLR Fach. Symp. der AG ATAB.*
- [18] Vio, G., Watkins, S., Mousley, P., Watmuff, J. and Prasad, S. 2005. Flow structures in the near-wake of the Ahmed model. *J Fluid Struct.* 20(5): 673-695.

- [19] Cheng, S.Y., Tsubokura, M., Nakashima, T., Nouzawa, T., and Okada, Y. 2011. A numerical analysis of transient flow past road vehicles subjected to pitching oscillation. *J Wind Eng Ind Aerod.* 99: 511-522.
- [20] Cheng, S.Y., Tsubokura, M., Nakashima, T., Okada, Y. and Nouzawa, T. 2012. Numerical quantification of aerodynamic damping on pitching of vehicle-inspired bluff body. *J Fluid Struct.* 30: 188-204.